Formation of ettringite, $Ca_6Al_2(SO_4)_3(OH)_{12} \cdot 26H_2O$, AFt, and monosulfate, $Ca_4Al_2O_6(SO_4) \cdot 14H_2O$, AFm-14, in hydrothermal hydration of Portland cement and of calcium aluminum oxide—calcium sulfate dihydrate mixtures studied by in situ synchrotron X-ray powder diffraction

Axel Nørlund Christensen,[a,1] Torben R. Jensen,[a,*] and Jonathan C. Hanson[b]

[a] Department of Chemistry, University of Aarhus, Langelandsgade 140, Aarhus C DK-8000, Denmark
[b] Chemistry Department, Brookhaven National Laboratory, Upton, NY 11973, USA

Abstract

In the hydration of calcium aluminum oxide–gypsum mixtures, i.e., $Ca_3Al_2O_6$, $Ca_{12}Al_{14}O_{33}$ and $CaSO_4 \cdot 2H_2O$, the reaction products can be ettringite, $Ca_6Al_2(SO_4)_3(OH)_{12} \cdot 26H_2O$, monosulfate, $Ca_4Al_2O_6(SO_4) \cdot 14H_2O$, or the calcium aluminum oxide hydrate, $Ca_4Al_2O_7 \cdot 19H_2O$. Ettringite is formed if sufficient $CaSO_4 \cdot 2H_2O$ is present in the mixture. Ettringite is converted to monosulfate when all $CaSO_4 \cdot 2H_2O$ is consumed in the synthesis of ettringite. The reactions were investigated in the temperature range 25–170°C using in situ synchrotron X-ray powder diffraction. This technique allows the study of very fast chemical reactions that are observed here under hydrothermal conditions. A new experimental approach was developed to perform in situ mixing of the reactants during X-ray data collection.
© 2004 Elsevier Inc. All rights reserved.

1. Introduction

The hydration of cements is a sequence of chemical reactions between solid compounds and water, leading to setting and hardening of the cement–water mixtures. The ettringites are formed in the early stages of Portland cement hydration by the reaction of the aluminate phases, calcium sulfate and water. Sulfate, carbonate and hydroxide ettringites are known and the compositions of their solid solutions have been investigated [1,2]. Calcium sulfate ($CaSO_4 \cdot 2H_2O$ and $CaSO_4 \cdot 0.5H_2O$) reacts with $Ca_3Al_2O_6$ (C_3A) at room temperature to form the calcium trisulfoaluminate hydrate known as sulfate ettringite, $Ca_6Al_2(SO_4)_3(OH)_{12} \cdot 26H_2O$ (AFt) [3,4]. In similar ways, carbonate ettringite and hydroxy ettringite are made using calcium carbonate, $CaCO_3$, or calcium oxide, CaO, as reactants [2].

The crystalline products formed in C_3A hydration are the metastable compounds $Ca_2Al_2O_5 \cdot 8H_2O$, C_2AH_8, and hydrocalumite, $Ca_4Al_2(OH)_{14} \cdot 6H_2O$, C_4AH_{13}, which have layer structures, where the water content can be as high as corresponding to $Ca_4Al_2O_7 \cdot 19H_2O$, C_4AH_{19} [4]. Hydration of C_3A in the presence of gypsum, $CaSO_4 \cdot 2H_2O$, results in formation of ettringite. After 8–16 h or even more as gypsum becomes increasingly consumed, hydrocalumite will be formed in significant amounts [4], and ettringite will react with hydrocalumite to a calcium monosulfatoaluminate hydrate, $Ca_4Al_2(SO_4)(OH)_{12} \cdot 6H_2O$ or $Ca_4Al_2O_6(SO_4) \cdot 12H_2O$, monosulfate [4]. The formation of monosulfate at 25°C takes 8–11 days [5].

Cement hydration at 70–100°C shows that no ettringite is present after several hours at 70°C, no monosulfate is present after several hours at 100°C, and that C_3AH_6 is observed as the product in the temperature range 80–110°C [6,7].

Investigation of the hydration processes of cement was typically carried out ex situ on reaction products

*Corresponding author. Fax: +001-45-8619-6199.

E-mail address: trj@chem.au.dk (T.R. Jensen).

[1] Present address: Højkolvej 7, DK-8210 Aarhus V, Denmark.

where the reactions had been stopped in some way. Information at realistic synthetic conditions can be obtained by time-resolved in situ studies that obviate the necessity of extrapolation from experimental to ambient conditions and remove artifacts as phase or composition changes induced in ex situ investigations. The pioneering in situ powder neutron diffraction investigations of the hydration of calcium aluminates with D_2O [8] and the studies of ettringite formations [9] are examples of this approach. The latter investigation showed that a precursor phase was formed prior to the formation of sulfate ettringite. Using time-resolved synchrotron energy dispersive technique, the synthesis of ettringite during mine packing was studied [10] and the onset of decomposition of ettringite at $114 \pm 1°C$ was reported [11]. The formation of sulfate ettringite at 20°C has been investigated using time-resolved synchrotron angle dispersive technique. It was found that gypsum was consumed during 3 h in the formation of sulfate ettringite, and when all gypsum was consumed, the hydration of the calcium aluminate phases produced the hydrate C_2AH_8 [12].

It was decided to study the formation of sulfate ettringite in hydrothermal hydration of calcium aluminates using time-resolved synchrotron angle dispersive techniques, and to reinvestigate the powder neutron diffraction data [9] to see if formation of a precursor phase prior to the formation of sulfate ettringite was real, and to determine the thermal persistence of sulfate ettringite. The purpose of the investigation was not to further study the phase stability of ettringite [11] but rather to investigate how ettringite and monosulfate react at hydrothermal conditions. The application of hydrothermal experimental conditions is relevant to cement chemistry, as one of many tests of physical properties of concrete castings is an autoclave treatment of the samples prior to the physical tests. The results of the present investigation are reported below.

2. Experimental

2.1. Chemistry

Aluminum hydroxide hydrate, $Al(OH)_3 \cdot xH_2O$ (Aldrich), calcium carbonate, $CaCO_3$ (Merck), calcium sulfate dihydrate, $CaSO_4 \cdot 2H_2O$, gypsum (precipitated, Riedel de Haën), and sodium hydrogen carbonate, $NaHCO_3$ (Merck), were used in the sample preparations. The composition of $Al(OH)_3 \cdot xH_2O$ was determined in a gravimetric analysis where a sample of the compound placed in a platinum crucible was heated to 1200°C for 25 h. The measured weight loss of 46.4% corresponds to the composition $Al(OH)_3 \cdot 0.949H_2O$. The calcium aluminum oxides C_3A and $Ca_{12}Al_{14}O_{33}$ ($C_{12}A_7$) were made from stoichiometric mixtures of

Table 1
Composition of calcium aluminum oxide–$CaSO_4 \cdot 2H_2O$ mixtures

Sample	Calcium aluminum oxide	$CaSO_4 \cdot 2H_2O$, w/w (%)	Al^{3+}/SO_4^{2-} (mole ratio)
A	C_3A	9.87	11.62
B	C_3A (Na^+ doped)[a]	9.84	11.63
C	$C_{12}A_7$	9.92	15.78
D	$C_{12}A_7$	37.00	2.96

[a] Nominal composition $Na_{0.36}Ca_{2.82}Al_2O_6$.

$Al(OH)_3 \cdot 0.949H_2O$ and $CaCO_3$. The powders were mixed and pressed into 39 mm diameter and 3 mm thick tablets in a mould of cemented carbide and the tablets were heated in platinum crucibles in an electric furnace at 1300°C for 72 h. The tablets were heated twice with an intermediate grinding to ensure homogeneity. The grinding was performed using a boron carbide mortar and the products were passed through a 0.112 mm sieve and stored in airtight plastic flasks at room temperature. Phase purity of the products was estimated from their powder X-ray diffraction patterns. An attempt to make an orthorhombic C_3A as Na^+ ion doped C_3A in the solid state synthesis resulted in a product with the nominal composition $Na_{0.36}Ca_{2.82}Al_2O_6$. This sample had a minor impurity of $C_{12}A_7$.

The calcium aluminum oxide–calcium sulfate dihydrate mixtures were ground for 5 min in a boron carbide mortar and stored in airtight plastic flasks. The calcium sulfate dihydrate sample was a precipitated sample which could pass through a 0.112 mm sieve. As calcium sulfate dihydrate is less hard than the calcium aluminum oxides, it is assumed that after the grinding it also has a comparable or even smaller grain size than the calcium aluminates. The gypsum wt% and the Al^{3+}/SO_4^{2-} ratios of the mixtures are listed in Table 1. The mole ratio must be as low as 2.00 for a theoretical conversion of all aluminum present in the sample to monosulfate, and as low as 0.67 for a complete conversion of all aluminum to ettringite. None of the samples have that low mole ratio which suggest that other reaction products than monosulfate and ettringite also may be formed. The sample of the industrial product White Portland Cement from Aalborg Portland A/S, Denmark, had the composition (as oxides): SiO_2: 24.7%, Al_2O_3: 1.74%, Fe_2O_3: 0.31%, CaO: 69.13%, MgO: 0.56%, SO_3: 1.97%, K_2O: 0.05%, Na_2O: 0.35%, loss in ignition: 0.99%, total: 99.80%. Free CaO: 2.22% and Al^{3+}/SO_4^{2-} mole ratio: 1.39.

2.2. Powder X-ray diffraction

Powder diffraction patterns for phase identifications were measured at room temperature on a Stoe Stadi diffractometer using transmission geometry with the samples on Scotch tape. The diffractometer had a curved Ge (111) monochromator yielding $CuK\alpha_1$

radiation ($\lambda = 1.540598$ Å) and a linear position-sensitive detector covering 5° in 2θ. A step scan mode was used where the recording time for a pattern covering 70° in 2θ was typically 21 h. The diffractometer was calibrated with an external Si standard ($a_{Si} = 5.43050$ Å). The diffractometer also had a position-sensitive detector covering 40° in 2θ.

2.3. Time-resolved hydrothermal reactions

The time-resolved synchrotron X-ray diffraction data were collected on the beam line X7B of the National Synchrotron Light Source using a MAR345 area detector. The samples were placed in 0.7 mm diameter quartz glass capillaries and heated with hot air. The solid sample was placed at the tip of the 0.7 mm diameter capillary with a height not exceeding 1 mm. Water was placed in the capillary with a syringe using a 0.5 mm quartz glass capillary as needle. The quantity of water corresponded typically to a length of 10 mm in the 0.7 mm diameter capillary. The water:solid ratio was thus typically 10:1. The water contained less than 0.1% of a detergent, which reduces the surface tension considerably and causes an immediate wetting of the solid sample when in contact with water. When this was the case before the diffraction measurements started, the sample is called a moist mixture, see below. Prior to the experiments, the phase transition and melting point of an S_8 powder was measured to calibrate the sample temperature. The results showed a good agreement between the actual and measured sample temperature (melting of sulfur observed at 120°C, mp(S_8) = 119°C). The temperature of the hot air flow was measured with a chromel–alumel thermocouple placed approximately 2 mm from the capillary. Temperature ramps from 25°C to 120°C and from 25°C to 170°C were used with heating rates of 0.79 and 1.21°C/min, respectively. The recording time for a pattern in the two temperature ramps were 1.41 and 2.45 min, corresponding to a temperature increase during the recording of a pattern of 1.11°C and 2.96°C/pattern, respectively. An internal pressure in the capillaries of up to 1700 kPa from a nitrogen gas cylinder ensured that water vapor bubbles did not form in the hydrothermal liquid. This marginal increase in pressure from ambient pressure to 1700 kPa will have a negligible effect on the formation or decomposition of phases in the sample since solids and liquids are highly incompressible and the free-energy surface is almost flat in the pressure direction for condensed systems. The capillaries were oscillated 10° to randomize the orientations of the crystallites in the samples. The wavelength used was $\lambda = 0.92018$ Å measured from a powder pattern of LaB_6 ($a = 4.1570$ Å). LaB_6 works in addition as an external standard in the calibration of the diffractometer, i.e., refinement of wavelength, detector orientation, beam

center and detector to sample distance. The MAR345 area detector recorded frames with Bragg diffraction rings and with diffraction spots from crystallites in the samples. The diffraction data on the frames were converted to powder patterns with the software FIT2D [13,14]. The powder patterns measured with the MAR345 detector are in the 2θ range 0–38°, with $(\sin\theta/\lambda)_{max} = 0.354$. To make the low 2θ range more detailed in the figures displayed below, only a selected part of the measured 2θ range is used for these figures. However, the whole ranges were used for phase identification of the reaction products observed in the in situ measurements.

2.3.1. Sample A, C_3A–gypsum–H_2O mixture

Fig. 1 displays patterns from the hydrothermal reactions of the sample heated from 25°C to 120°C. The sample was a moist mixture made approximately 5 min before the first pattern was recorded at 25°C. C_3A is the most reactive of the calcium aluminum oxides investigated [8]. The intensity of the 020 gypsum reflection at $2\theta = 6.91°$ ($d = 7.63$ Å) (JCPDS card No. 33–311) decreases slowly, and the compound is not present after pattern No. 33 at 62°C. Two intermediate phases are formed immediately, one with strong reflections at $2\theta = 4.91°$ ($d = 10.7$ Å), and $2\theta = 9.75°$ ($d = 5.41$ Å), and one with $2\theta = 5.44°$ ($d = 9.70$ Å), and $2\theta = 10.95°$ ($d = 4.82$ Å), corresponding to the compounds C_4AH_{19} (JCPDS card No. 14–628), and
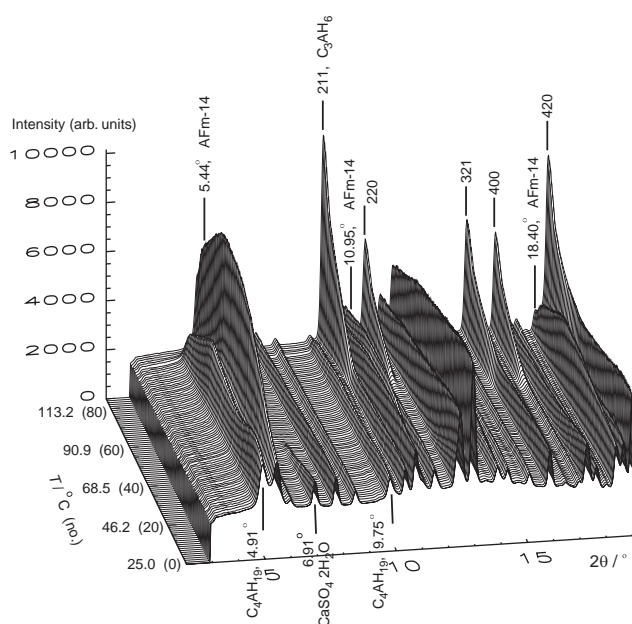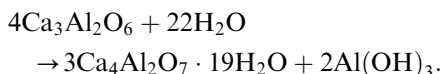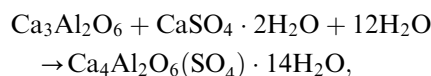

Fig. 1. Stack of powder patterns of sample A, a C_3A–gypsum–H_2O mix, hydrated in a temperature ramp from 25°C to 120°C, and recorded using synchrotron radiation, $\lambda = 0.92018$ Å. The reflections at $2\theta = 4.91°$ and 9.75° belong to C_4AH_{19}, those at $2\theta = 5.44°$, 10.95° and 18.40° belong to AFm-14, and the reflection at $2\theta = 6.91°$ is the 0 2 0 reflection of $CaSO_4 \cdot 2H_2O$. Positions of C_3AH_6 reflections are marked with Miller indices.

$Ca_4Al_2O_6(SO_4) \cdot 14H_2O$, AFm-14, (JCPDS card No. 42–62), respectively. The choice between C_4AH_{19} and C_2AH_8 for the product with the reflections at $2\theta = 4.91°$ and $9.75°$ is made considering the observed intensity ratio between the two reflections of 100/30. The two published powder patterns of C_2AH_8 (JCPDS No. 11–205 and No. 45–564) have an average ratio of the intensities of the two reflections of 100/76 and the published powder pattern of C_4AH_{19} (JCPDS card No. 14–628) has an average of the intensities of the two reflections of 100/31. The quantity of C_4AH_{19} has its maximum in pattern No. 56 (87°C) and the compound is completely consumed in pattern No. 83 (117°C). The quantity of AFm-14 has its maximum in pattern No. 60 (92°C) but the compound is still present in the last pattern, No. 86 (120°C). The end product of the hydration $Ca_3Al_2(OH)_{12}$, C_3AH_6 (JCPDS card No. 24–217) is observed from pattern No. 54 (85°C) and grows coupled to the depletion of C_4AH_{19}. Its growth is accelerated when AFm-14 starts to be consumed. Ettringite is not observed in this experiment. The chemical reactions are

$$Ca_3Al_2O_6 + CaSO_4 \cdot 2H_2O + 12H_2O$$
$$\rightarrow Ca_4Al_2O_6(SO_4) \cdot 14H_2O,$$

$$4Ca_3Al_2O_6 + 22H_2O$$
$$\rightarrow 3Ca_4Al_2O_7 \cdot 19H_2O + 2Al(OH)_3.$$

2.3.2. Sample B, Na-doped C_3A–gypsum–H_2O mixture

The solid sample contains orthorhombic C_3A with an impurity of $C_{12}A_7$. Fig. 2 displays patterns from the hydrothermal reactions of the mix heated from 25°C to 120°C. The sample was a moist mixture made approximately 5 min before the first pattern recorded at 25°C. The first pattern has reflections from ettringite, AFt, (JCPDS card No. 41–1451), gypsum, and C_3A. Gypsum is consumed and is not present after pattern No. 18 (45°C). The ettringite reflections at $2\theta = 5.41°$ ($d = 9.75$ Å) and $2\theta = 9.38°$ ($d = 5.63$ Å) increase in intensity up to pattern No. 19 (46°C) and ettringite is not present after pattern No. 39 (68°C). A weak reflection of C_4AH_{19} is observed in the patterns No. 17–21 (44–48°C), and simultaneously the reflection at $2\theta = 5.41°$ (ettringite) is shifted to $2\theta = 5.50°$, indicating that AFm-14 grows in depletion of ettringite. The second hydration product C_3AH_6 is observed from pattern No. 55 (86°C). C_3A is present in all the patterns. The reactions are
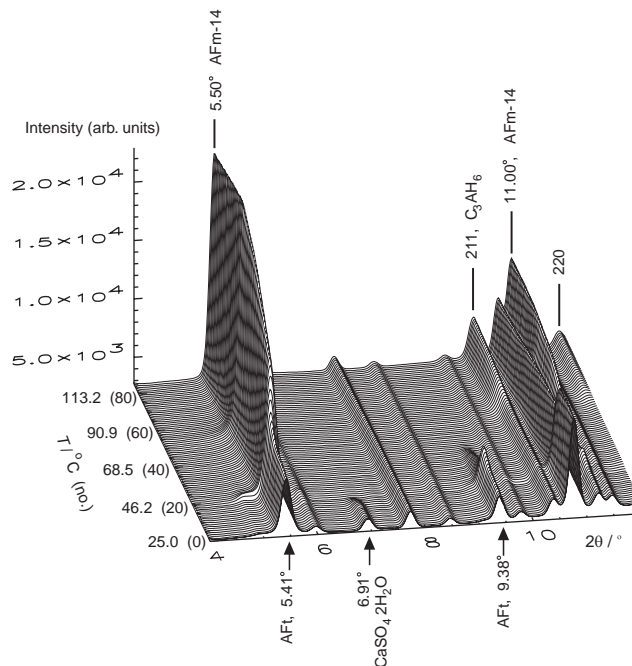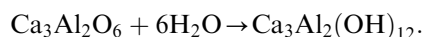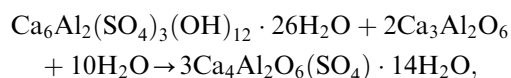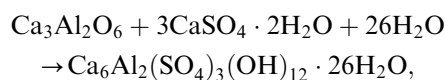
$$Ca_3Al_2O_6 + 3CaSO_4 \cdot 2H_2O + 26H_2O$$
$$\rightarrow Ca_6Al_2(SO_4)_3(OH)_{12} \cdot 26H_2O,$$

$$Ca_6Al_2(SO_4)_3(OH)_{12} \cdot 26H_2O + 2Ca_3Al_2O_6$$
$$+ 10H_2O \rightarrow 3Ca_4Al_2O_6(SO_4) \cdot 14H_2O,$$

$$Ca_3Al_2O_6 + 6H_2O \rightarrow Ca_3Al_2(OH)_{12}.$$

Fig. 2. Stack of powder patterns of sample B, a mix of Na^+ doped C_3A–gypsum–H_2O hydrated in a temperature ramp from 25°C to 120°C, $\lambda = 0.92018$ Å. Reflections of $2\theta = 5.41°$ and $9.38°$ belong to ettringite, AFt, the reflection at $2\theta = 6.92°$ to $CaSO_4 \cdot 2H_2O$ and the reflections at $2\theta = 5.50°$ and $11.00°$ belong to AFm-14. Positions of C_3AH_6 are marked with Miller indices. The hydration path for sample B is thus different from that of sample A.

2.3.3. Sample C, $C_{12}A_7$–gypsum–H_2O mixture

This sample contains $C_{12}A_7$ which has a slower hydration reaction than C_3A [8]. Fig. 3 displays patterns from the hydrothermal reactions in the temperature range 25–170°C. The mixture was made approximately 5 min before the first pattern was recorded. The patterns No. 1–13 (25–65°C) show that the quantity of ettringite, AFt, increases, and that gypsum is consumed. A very fast chemical reaction is observed, and pattern No. 14 (68°C) is completely different from the previous pattern. In the temperature range 65–68°C, all ettringite and all gypsum is converted to C_4AH_{19} and AFm-14 and an amorphous phase, possibly aluminum hydroxide, observed as an increase in the background at $2\theta = 1.5°$. C_4AH_{19} is present up to pattern No. 23 (96°C), and AFm-14 increases in quantity to pattern No. 24 (99°C) and is completely consumed in the last pattern at 170°C. From pattern No. 18 (80°C), the hydration product C_3AH_6 forms and increases in quantity to the end temperature 170°C. An additional phase is formed and seen in patterns 44–49 (161–170°C) with $2\theta = 8.50°$ ($d = 6.21$ Å). This is most likely $CaSO_4 \cdot 0.5H_2O$ which can be formed at hydrothermal conditions. This also explains that the amorphous background at $2\theta = 1.5°$ is increased additionally as aluminum hydroxide is formed in the depletion of
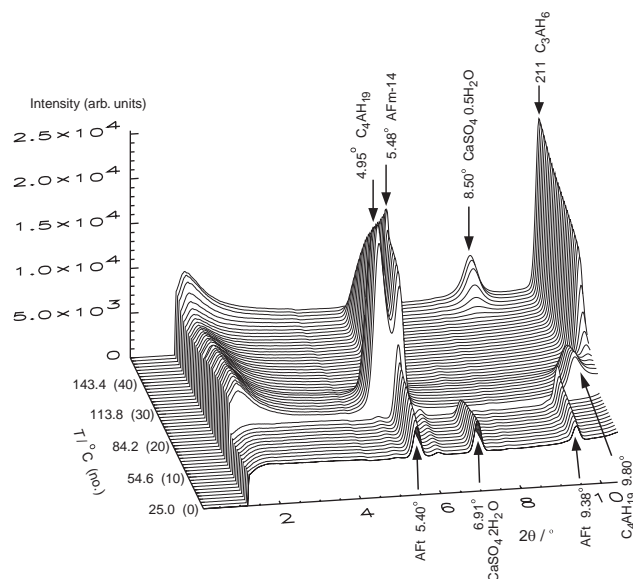
Fig. 3. Stack of powder patterns of sample C, a $C_{12}A_7$–gypsum–H_2O mix, hydrated in a temperature ramp from 25°C to 170°C, $\lambda = 0.92018$ Å. Reflections at $2\theta = 5.40°$ and 9.38° belong to ettringite, AFt, the $CaSO_4 \cdot 2H_2O$ reflection is at 6.91°, the reflections at $2\theta = 4.95°$ and 9.8° belong to C_4AH_{19}, the reflection at $2\theta = 5.48°$ belong to AFm-14, and the reflection at $2\theta = 8.50°$ is the 2 0 0 reflection of $CaSO_4 \cdot 0.5H_2O$. The position of a C_3AH_6 reflection is marked with Miller indices.
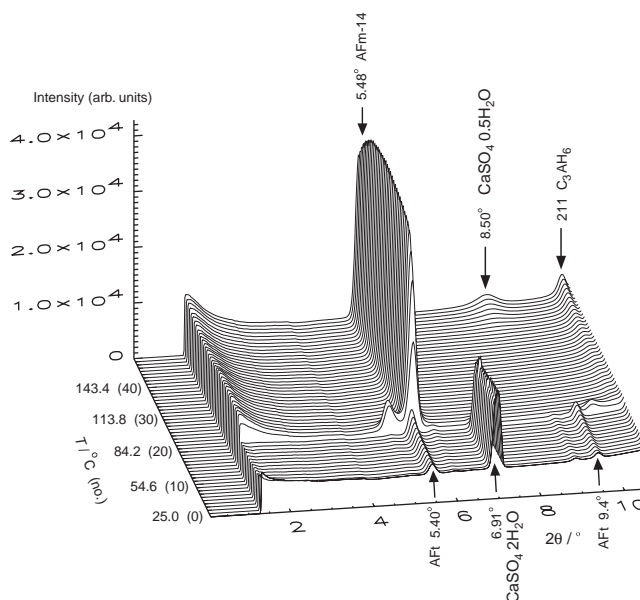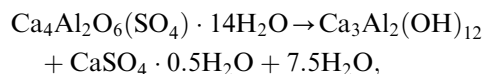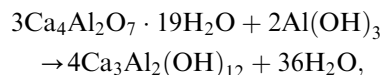

Fig. 4. Stack of powder patterns of sample D, a $C_{12}A_7$–gypsum–H_2O mix, with a high content of gypsum, hydrated in a temperature ramp from 25°C to 170°C, $\lambda = 0.92018$ Å. Reflections at $2\theta = 5.4°$ and 9.4° belong to ettringite, AFt, at $2\theta = 6.9°$ to $CaSO_4 \cdot 2H_2O$, the reflection at $2\theta = 5.48°$ belongs to AFm-14 and that at $2\theta = 8.50°$ belongs to $CaSO_4 \cdot 0.5H_2O$. The position of a C_3AH_6 reflection is marked with Miller indices.
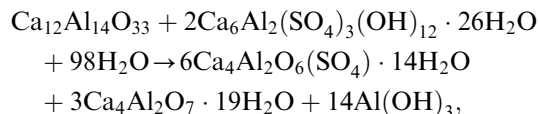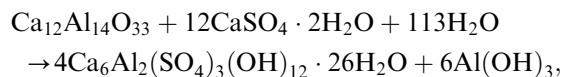
$C_{12}A_7$. The reactions are

$$Ca_{12}Al_{14}O_{33} + 12CaSO_4 \cdot 2H_2O + 113H_2O$$
$$\rightarrow 4Ca_6Al_2(SO_4)_3(OH)_{12} \cdot 26H_2O + 6Al(OH)_3,$$

$$Ca_{12}Al_{14}O_{33} + 2Ca_6Al_2(SO_4)_3(OH)_{12} \cdot 26H_2O$$
$$+ 98H_2O \rightarrow 6Ca_4Al_2O_6(SO_4) \cdot 14H_2O$$
$$+ 3Ca_4Al_2O_7 \cdot 19H_2O + 14Al(OH)_3,$$

$$3Ca_4Al_2O_7 \cdot 19H_2O + 2Al(OH)_3$$
$$\rightarrow 4Ca_3Al_2(OH)_{12} + 36H_2O,$$

$$Ca_4Al_2O_6(SO_4) \cdot 14H_2O \rightarrow Ca_3Al_2(OH)_{12}$$
$$+ CaSO_4 \cdot 0.5H_2O + 7.5H_2O,$$

$$Ca_{12}Al_{14}O_{33} + 33H_2O \rightarrow 4Ca_3Al_2(OH)_{12} + 6Al(OH)_3.$$

2.3.4. Sample D, $C_{12}A_7$–gypsum–H_2O mixture

This sample has a high content of gypsum. Fig. 4 displays patterns from the hydrothermal reactions in the temperature range 25–170°C. The sample was a moist mix made 10 min before the first pattern was recorded. Patterns No. 1–14 (25–68°C) show that gypsum is present, almost unchanged in quantity, and that ettringite, AFt, is present in increasing quantity. A very fast chemical reaction is observed, and pattern No. 15 (71°C) is completely different from the previous pattern. In the temperature range 68–71°C, all ettringite and all gypsum are used up, C_4AH_{19} and AFm-14 are formed.

Simultaneously, the background at $2\theta = 1.5°$ is increased considerably, indicating formation of an amorphous phase, possibly aluminum hydroxide, coupled with a drastic reduction in the quantity of solid $C_{12}A_7$, not shown in the figure. C_4AH_{19} is only present in two patterns, No. 15–16 (71–74°C). AFm-14 is present up to 170°C. The Al^{3+}/SO_4^{2-} mole ratio 2.96 of the sample is close to the value 2.00 for a theoretical conversion of all aluminum present in the sample to monosulfate and considerably smaller than the ratio 15.78 in sample C. This explains why C_4AH_{19} is present only as a minor quantity compared to that observed in the sample C experiment. C_3AH_6 is observed from pattern No. 25 (100°C).

2.3.5. Aalborg Portland cement–H_2O mixture

The sample is a white Portland cement with a low content of gypsum. Fig. 5 displays the patterns from the hydration reaction in the temperature range 25–120°C. The dry solid is mixed with water after the first diffraction pattern was recorded. This explains the shift in background from pattern No. 1–2. Ettringite is slowly forming until pattern No. 21 (48°C). This is possibly more clearly observed in Fig. 6 which displays patterns No. 10–85 in the 2θ range 4.0–8.5°. The 100 ettringite, AFt, reflection is observed at $2\theta = 5.43°$ ($d = 9.71$ Å). At the temperature 48°C, the conversion of ettringite to AFm-14 starts, and the typical reflections for this
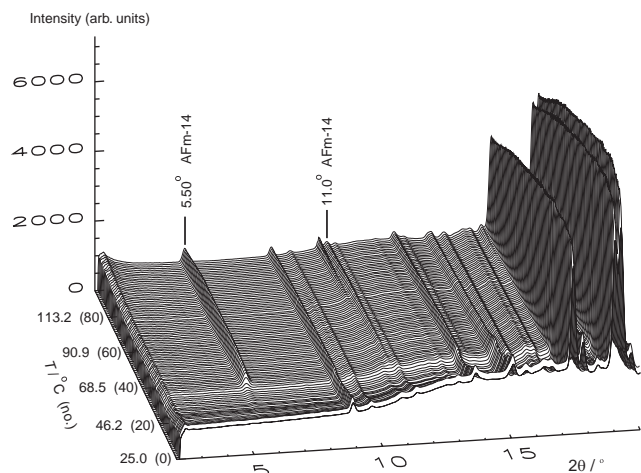
Fig. 5. Stack of powder patterns of the Portland cement–H$_2$O mix, hydrated in a temperature ramp from 25°C to 120°C, $\lambda = 0.92018$ Å. The reflections at $2\theta = 5.50°$ and 11.0° belong to AFm-14.
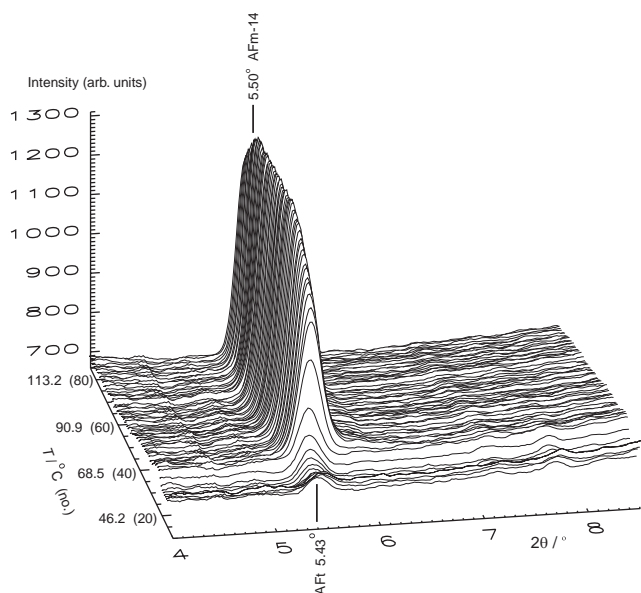

Fig. 6. Stack of the powder patterns No. 10–85 in the 2θ range 4.0–8.5° of the same patterns as displayed in Fig. 5. The reflection at $2\theta = 5.43°$ belongs to ettringite, AFt, and the reflection at $2\theta = 5.50°$ belongs to AFm-14.

compound at $2\theta = 5.49°$ ($d = 9.61$ Å), and $2\theta = 11.05°$ ($d = 4.78$ Å) are observed.

3. Results and discussions

The thermal decomposition temperature for the reaction of ettringite to monosulfate was determined to 110°C in a differential scanning calorimetry investigation [15]. The thermal decomposition temperature of ettringite under hydrothermal conditions was found to be $111 \pm 1°$C [16] and $114 \pm 1°$C [11], respectively. These

investigations were made on pure crystalline ettringite. However, in the synthesis of ettringite in aqueous solutions of C$_3$A and gypsum, ettringite was obtained up to 90°C, but the reaction was at high temperature retarded and not quantitative [17]. This investigation was made with a C$_3$A/gypsum molar ratio 1/3.3, which is sufficient to convert all C$_3$A to ettringite. The present investigation shows that the conditions for having ettringite as a reaction product in the hydration of C$_3$A–gypsum–H$_2$O, and C$_{12}$A$_7$–gypsum–H$_2$O mixtures are temperature dependent and also composition dependent. With the reactive C$_3$A in the mixture, sample A, ettringite was not observed but could possibly have been formed if the mixture had contained more gypsum. It has been observed in Portland cement hydration reactions, that ettringite, monosulfate and gypsum can be present simultaneously [18]. With the Na$^+$ doped C$_3$A containing orthorhombic C$_3$A with an impurity of C$_{12}$A$_7$, sample B, and with C$_{12}$A$_7$, samples C and D, in the mixtures, ettringite was observed at temperatures up to 68°C. It is well known that ettringite may form rapidly [19]. The reaction products AFm-14 and C$_4$AH$_{19}$ formed at the depletion of ettringite. Their relative quantity depends upon the amount of gypsum available, and this then limits the temperature ranges where C$_4$AH$_{19}$ was found. The compound AFm-14 was apparently stable at temperatures up to 170°C, the compound C$_3$AH$_6$ was typically formed at approximately 85°C and was stable up to 170°C. Ettringite was observed in the hydration of white Portland cement at temperatures up to 48°C and was then converted on further heating to AFm-14. In hydration of a Portland cement with a SO$_3$ content of 3.37 wt%, ettringite was observed in the temperature range 25–75°C [20]. A difference in the hydration of cubic and orthorhombic C3A has also been observed in hydration of the phases present in Portland cement clinker [20].

The results obtained in the investigations reported above inspired a reinvestigation of the pioneering in situ powder neutron diffraction work by Christensen et al. [9] of the hydration of a C$_{12}$A$_7$–CaSO$_4 \cdot$2D$_2$O–D$_2$O mixture, which was the first in situ diffraction study within cement research [8,9]. A sample containing 37.7 wt% CaSO$_4 \cdot$2D$_2$O was used [9], which is comparable to the composition of sample D (Table 1). The hydration proceeded at the constant temperature 27°C, and showed the formation of one phase which in a short span of time (3 h) was partly converted to a second phase. These results were at that time interpreted as formation of a precursor phase for ettringite [9]. The first phase was shown to have unit cell parameters of a hexagonal cell $a = 11.19(1)$, $c = 21.42(4)$ Å, rather close to the values of the unit cell parameters for ettringite. The indexing of the Bragg reflections in the powder neutron diffraction patterns was hampered by the lack of a database for powder neutron diffraction patterns
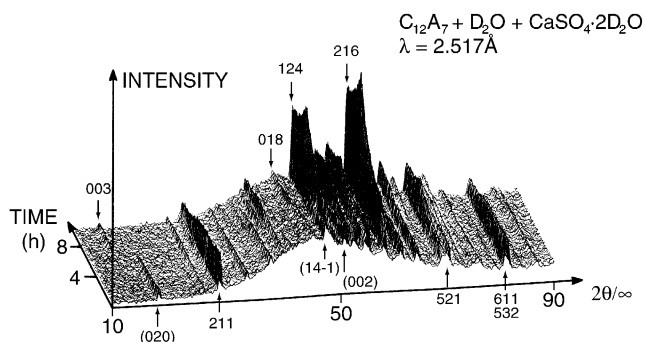
Fig. 7. Stack of powder patterns of a $C_{12}A_7$–$CaSO_4 \cdot 2D_2O$–D_2O mix, hydrated at 27°C and recorded on the neutron powder diffractometer D1B using $\lambda = 2.517 \text{ Å}$ neutrons (9). Some of the strong $C_{12}A_7$ reflections at $2\theta = 29.9°$, 70.3°, and 80.8° are marked with the Miller indices 2 1 1, 5 2 1, 6 1 1, and 5 3 2. Some of the stronger $CaSO_4 \cdot 2D_2O$ reflections at $2\theta = 19.1°$, 48.5° and 52.1° are marked with Miller indices in brackets, 0 2 0, 1 4 $\bar{1}$, and 0 0 2. In the upper part of the figure, two of the stronger ettringite reflections at $2\theta = 49.0°$ and 58.7° are marked with their Miller indices 1 2 4 and 2 1 6, and two reflections from $Ca_4Al_2O_6(SO_4) \cdot 14D_2O$ at $2\theta = 15.3°$ and 51.2° are marked with their Miller indices 0 0 3 and 0 1 8, respectively.
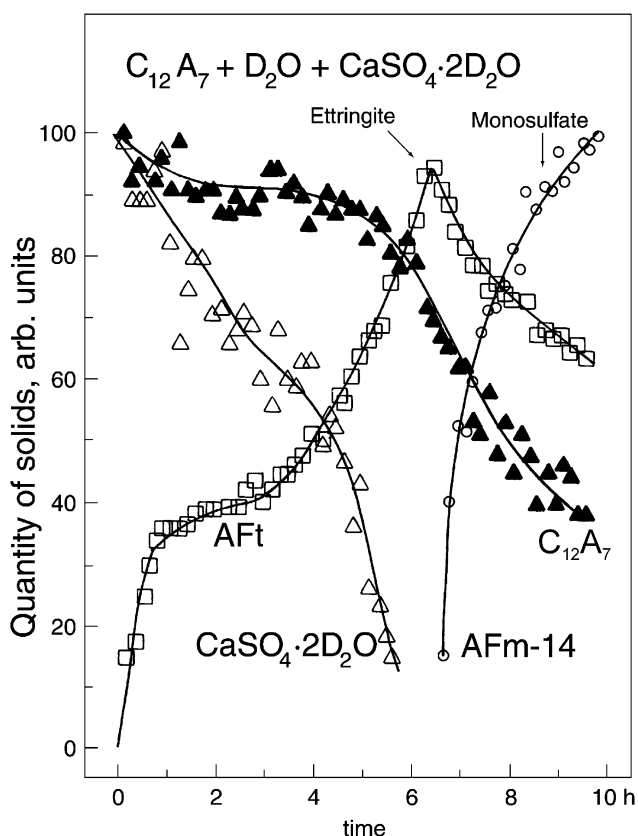

Fig. 8. Quantity of solids, normalized, and calculated from integrated Bragg reflections of $C_{12}A_7$, $CaSO_4 \cdot 2D_2O$, ettringite and monosulfate at 27°C.

with intensities of the Bragg reflections of deuterated samples of pure ettringite and pure monosulfate. The interpretation [9] is in error so that the first phase

formed was indeed ettringite and that this was in time converted to $Ca_4Al_2O_6(SO_4) \cdot 14D_2O$ similar to the in situ experiments reported above.

Fig. 7 displays a stack of powder neutron diffraction patterns of a $C_{12}A_7$–$CaSO_4 \cdot 2D_2O$–D_2O mix hydrated at 27°C and recorded in 1982 at the instrument D1B, Institut Laue-Langevin, Grenoble, using $\lambda = 2.517 \text{ Å}$ neutrons [9]. Miller indices for the solids present in the experiment are indicated. Fig. 8 shows that the depletion of $CaSO_4 \cdot 2D_2O$ is coupled with the growth of the first product AFt. When all $CaSO_4 \cdot 2D_2O$ is used, the depletion of ettringite starts and the second product monosulfate, $Ca_4Al_2O_6(SO_4) \cdot 14D_2O$, AFm-14, is formed. This is exactly the same sequence of reactions as observed and reported above, Fig. 3.

4. Conclusion

Ettringite is formed in hydration of calcium aluminum oxide–gypsum–water mixtures if sufficient gypsum is present relative to the quantity of reactive or soluble calcium aluminum oxide for its formation. If this is not the case, already formed ettringite will be converted to monosulfate when gypsum has been consumed. This was observed in very fast chemical reactions. In the case of the reactive C_3A and an insufficient quantity of gypsum in the mix, the monosulfate was formed directly. In all the experiments, the monosulfate formed was AFm-14. The intermediate aluminum oxide hydrate phase was identified as C_4AH_{19}.

References

[1] H. Poellmann, H.-J. Kuzel, Cement Concrete Res. 20 (1990) 941.

[2] S.J. Barnett, C.D. Adam, A.R.W. Jackson, Cement Concrete Res. 31 (2001) 13.

[3] J. Bensted, in: J. Bensted, P. Barnes (Eds.), Structure and Performance of Cement, Spon Press, London, New York, 2002, p. 253.

[4] E.M. Gartner, J.F. Young, D.A. Damidot, I. Jawed, in: J. Bensted, P. Barnes (Eds.), Structure and Performance of Cement, Spon Press, London and New York, 2002, p. 57.

[5] P.W. Brown, J. Am. Ceram. Soc. 76 (1993) 2971.

[6] H.F.W. Taylor, C. Famy, K.L. Scrivener, Cement Concrete Res. 31 (2001) 683.

[7] C. Famy, K.L. Scrivener, H.F.W. Taylor, in: J. Bensted, P. Barnes (Eds.), Structure and Performance of Cement, Spon Press, London and New York, 2002, p. 282.

[8] A.N. Christensen, M.S. Lehmann, J. Solid State Chem. 51 (1984) 196.

[9] A.N. Christensen, H. Fjellvåg, M.S. Lehmann, Acta Chem. Scand. A 40 (1986) 126.

[10] M.N. Muhamad, P. Barnes, C.H. Fentiman, D. Häusermann, H. Pollmann, S. Rashid, Cement Concrete Res. 23 (1993) 267.

[11] C. Hall, P. Barnes, A.D. Billimore, A.C. Jupe, X. Turrillas, J. Chem. Soc., Faraday Trans. 92 (1996) 2125.

[12] C. Evju, S. Hansen, Cement Concrete Res. 31 (2001) 257.

[13] A.P. Hammersley, ESRF Internal Report, ESRF98HA01T, FIT2D V9, 129, Reference Manual V3.1, 1998.

[14] A.P. Hammersley, S.O. Svensson, M. Hanfland, A.N. Fitch, D. Häusermann, Two-dimensional detector software: from real detector to idealized image of two-theta scan, High Pressure Res. 14 (1996) 235.

[15] K. Ogawa, R. Roy, Cement Concrete Res. 11 (1981) 741.

[16] V. Satava, O. Veprek, J. Am. Ceram. Soc. 58 (1975) 357.

[17] W. Lieber, Zement-Kalk-Gips 16 (1963) 364.

[18] P. Barnes, S. Colston, B. Craster, C. Hall, A. Jupe, S. Jacques, J. Cockcroft, S. Morgan, M. Johnson, D. O'Connor, M. Bellotto, J. Synchrotron Radiat. 7 (2000) 167.

[19] P. Barnes, X. Turrillas, A.C. Jupe, S.L. Colston, D. O'Connor, R.J. Cernik, P. Livesey, C. Hall, D. Bates, R. Dennis, J. Chem. Soc., Faraday Trans. 92 (1996) 2187.

[20] A.N. Christensen, N.V.Y. Scarlett, I.C. Madsen, T.R. Jensen, J.C. Hanson, J. Chem. Soc., Dalton Trans. 8 (2003) 1529.